Negative hydrogen ion densities and drift velocities in a multicusp ion source

P. J. Eenshuistra, M. Gochitashvilii,[a] R. Becker, A. W. Kleyn, and H. J. Hopman
Association EURATOM-FOM, FOM-Institute for Atomic and Molecular Physics, Kruislaan 407, 1098 SJ Amsterdam, The Netherlands

(Received 5 June 1989; accepted for publication 4 August 1989)

We have determined densities of negative hydrogen ions in a discharge by a laser detachment technique. We measured the electron density, the electron temperature, and the positive ion density using a Langmuir probe. We also performed extraction measurements. Combination of H^- density measurements and extraction measurements yields information about the H^- drift velocity. It was found that the velocity scaled with the square root of the electron temperature. All measurements were done as a function of discharge voltage, discharge current, and gas pressure. The densities are compatible with a semiquantitative model in which H^- is produced by dissociative attachment of plasma electrons to vibrationally excited molecules and destroyed by wall collisions at very low pressure and collisions with H atoms, positive ions and/or hot thermal electrons at higher pressure.

I. INTRODUCTION

There is a strong interest in negative hydrogen ion sources generating intense neutral hydrogen beams for fusion applications.[1] Much research is directed towards the development of two different types of sources: the so-called hydrogen volume source and the surface conversion source. Advantages and disadvantages of both types are discussed in several publications.[2–4] In volume sources, dissociative attachment of plasma electrons to vibrationally excited molecules is regarded as the dominant production process of H^- (Ref. 5):

$$H_2(v'') + e \rightarrow H_2^- (^2\Sigma_u^+) \rightarrow H^- + H(1s). \quad (1)$$

The cross section of this reaction depends strongly on the vibrational quantum number v''.[6,7] Accordingly, it is expected that molecules with $v'' \geqslant 5$ are responsible for the production of H^- in a discharge. Other candidates for H^- production are dissociative attachment of plasma electrons to metastable molecules $(c^3\Pi_u^-)$,[5,8]

$$H_2(c^3\Pi_u^-) + e \rightarrow H_2^- (^2\Pi_u) \rightarrow H^- + H(2p) \quad (2)$$

and polar dissociation of molecules by primary electrons,[9]

$$H_2 + e_p \rightarrow H^- + H^+ + e. \quad (3)$$

The latter process can also take place with H_3^+ ions instead of H_2 molecules with a larger cross section.[9] A review on the formation of H^- and $H_2(v'')$ has been presented by Hiskes.[5]

In the present paper we discuss studies on negative ion formation, performed in a bucket-type volume source. We also determined the vibrational populations and the atomic density in this source. These are discussed in detail in a separate paper, which complements this work.[10,11]

The density of the negative hydrogen ions has been determined for the first time in such a discharge, using laser detachment of the H^- ions, by Bacal and Hamilton.[12] We present results on H^- densities, but contrary to these authors, we have used radiation of variable frequency to eliminate other sources of detached electrons than H^-. Apart from measuring the H^- density, we did perform Langmuir probe measurements in the discharge to obtain the electron density, the primary electron density, the positive ion density, and the electron temperature. A bucket source is often divided into two different regions by a magnetic dipole filter (see Fig. 1). The first region, containing the arc discharge is called the "driver." Here, energetic electrons are present that excite, ionize, and dissociate gas molecules. The second region is called the "extractor." In this region only slow thermal plasma electrons are present, because only these are able to diffuse through the magnetic field.[13] The absence of fast electrons means that the extra electron of H^- is not detached in collisions with these electrons. In our source the extractor section and the magnetic filter can be removed. Therefore, our source can be operated in two configurations. The first configuration of source operation is the one normally applied in volume sources, i.e., with magnetic filter present and with the frontplate at the same potential as the source body. In this configuration we performed extraction measurements in addition to density measurements. H^- density and H^- extraction measurements under the same conditions give information about the drift velocity of H^-. In the second configuration we measured n_H in the same bucket, but without magnetic filter and with the front plate on filament potential. The negative front plate serves the same purpose as the magnetic filter, namely to confine the primary electrons in the plasma. Therefore, we expect that the values of n_H in the second configuration are characteristic for those in the driver region. It further enables us to compare these measurements in the second configuration with the REMPI measurements performed by Eenshuistra and coworkers.[10,11,14]

In this paper, we extend our model of the discharge presented in a separate paper[10] in Sec. II. In this model, we use

[a] Physics Department, Tbilisi State University, Chavchavadze 3, 380028, USSR.

 0021-8979/90/010085-12$03.00

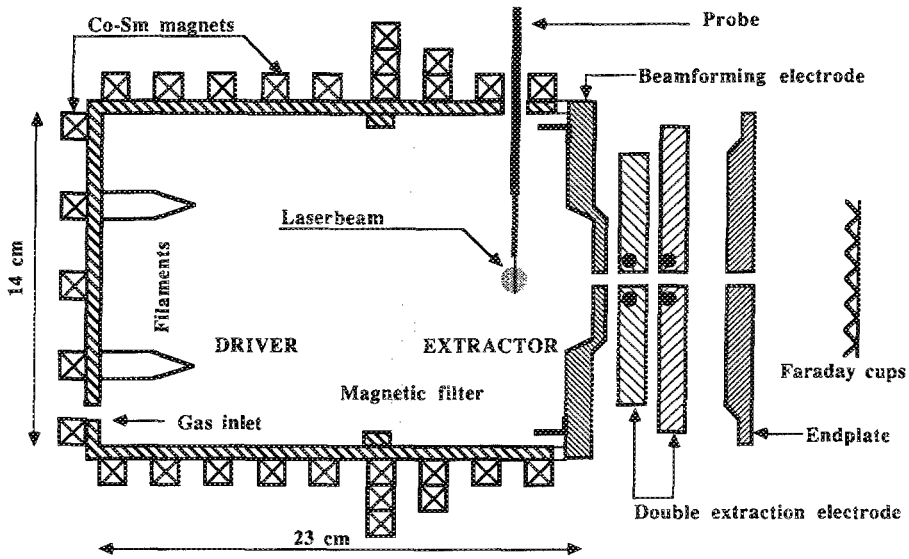

FIG. 1. Schematic top view of the source and the extraction system. Indicated are the magnetic filter, the probe, and the laser beam.

rate equations containing the processes that lead to the production and destruction of H^- ions in the source, such as wall and particle collisions. After introducing the experimental methods in Sec. III, we will present our measurements in Sec. IV, and discuss our results in terms of other data available in literature. In Sec. V, we discuss our results on the electron and H^- density in terms of the model of Sec. II. The conclusions will be summarized in Sec. VI.

II. MODEL FOR H^- FORMATION

Many reactions taking place in hydrogen volume sources and their cross sections have been reviewed recently by Hiskes.[5] Modeling by solving a set of coupled differential equations describing production and decay of all species in the discharge, using large computer codes, has been performed by Hiskes and co-workers[9,15,16] and Gorse *et al.*[17] Here we want to use analytical expressions that can give quick insight in the reactions concerned and that can describe our measurements qualitatively and sometimes quantitatively. In a separate paper we give the equations for H atoms and vibrationally excited molecules. Here we give the equations for primary electrons and positive ions. Plasma electrons are described by a similar expression as positive ions. After that we discuss the expressions for the negative ions.

We first consider the driver region. Primary electrons, accelerated from the filaments over the discharge voltage V_d, are the source for all excitation and ionization processes in the discharge. The characteristic loss time of primary electrons by inelastic collisions $\tau_{\rm in}$ is given by

$$\tau_{\rm in} = 1/n_g\langle\sigma_{\rm in} v_p\rangle, \tag{4}$$

where n_g denotes the gas density, $\sigma_{\rm in}$ the cross section for inelastic collisions, and v_p the average velocity of fast electrons. Following Goede and Green[18] and Leung *et al.*,[19] we write the following expression:

$$\frac{I_d}{eV} = n_p\left(\frac{1}{\tau_{\rm in}} + \frac{1}{\tau_w}\right), \tag{5}$$

where I_d denotes the discharge current, e the elementary electron charge, V the volume of the discharge, n_p the density of primary electrons, and τ_w the characteristic loss time of primary electrons by wall collisions. At low pressures, i.e., $p<0.3$ Pa,[11] the wall losses dominate, so $\tau_w < \tau_{\rm in}$. In this case n_p is proportional with discharge current. As $\tau_{\rm in}$ dominates over τ_w, then both density and energy distribution function of primary electrons are effected by n_g. From Eqs. (4) and (5) it is clear that n_p decreases with n_g at high pressures.

Many particles in the discharge are formed by inelastic collisions between gas molecules and primary electrons. Examples are plasma electrons with density n_e, metastable molecules,[14] hydrogen atoms with density $n_{\rm H}$, positive ions with density n_i, and vibrationally highly excited molecules $H_2(v'')$ with density n''. For positive ions we write:

$$n_i = n_g n_p \langle\sigma_{\rm ion} v_p\rangle \tau_i, \tag{6}$$

where τ_i denotes the average loss time of positive ions. Because we do not distinguish between H^+, H_2^+, and H_3^+ ions, this equation is correct in a global sense only. For thermal electrons one can write a similar expression. Substituting Eqs. (4) and (6) yields

$$n_i = \frac{I_d n_g \langle\sigma_{\rm ion} v_p\rangle \tau_i}{eV(n_g\langle\sigma_{\rm in} v_p\rangle + 1/\tau_w)}. \tag{7}$$

Equation (7) predicts that n_i will increase at low p with increasing p, when $1/\tau_w > n_g\langle\sigma_i v_p\rangle$ and saturate when $1/\tau_w < n_g\langle\sigma_i v_p\rangle n_i$. Equation (7) also predicts that n_i will increase with I_d. For the density of H^-, n_-, we write:

$$n_- = n'' n_e \langle\sigma_{\rm DA} v_e\rangle \tau_-, \tag{8}$$

with n'' the density of vibrationally excited molecules with $4 < v'' < 10$,[10] $\sigma_{\rm DA}$ the cross section for dissociative attachment, and v_e the velocity of plasma electrons. The loss processes of H^-, which we will discuss now, are applicable to both driver and extraction area. H^- can be destroyed by wall collisions, collisions with fast or thermally hot electrons ($T_e > 3$ eV, collisional detachment, cross section $\sigma_{\rm CD}$), and

collisions with discharge-produced particles such as atoms (associative detachment, cross section σ_{AD}):

$$H^- + H \rightarrow H_2^-(^2\Sigma_u) \rightarrow H_2(v'') + e, \tag{9}$$

and positive ions (mutual recombination, cross section σ_{MR})

$$H^- + H_x^+ \rightarrow H + \text{neutrals}. \tag{10}$$

The average loss time τ_- is given by

$$\tau_- = \frac{1}{v_-/L_- + n_p\langle\sigma_{CD}v_p\rangle + n_H\langle\sigma_{AD}v_H\rangle + n_i\langle\sigma_{MR}v_i\rangle}. \tag{11}$$

Loss by diffusion to the walls can be of importance at low pressure and/or low plasma density. Because in collisions of H^- with H_2 ($v'' = 0$) there is not enough energy available (0.75 eV) to detach the electron, this destruction process is not included in Eq. (11). The third term ($n_p\langle\sigma_{CD}v_p\rangle$) in the nominator of Eq. (11); destruction by primary electrons is of course only applicable in the driver region. The last two terms, destruction by atoms and ions, are candidates for loss of H^- in both the driver and extractor regions. In the driver, thermal electrons with an energy larger than 2 eV can also quench H^- (collisional detachment). This process can be included in the last term by increasing the rate coefficient, since electrons have the same density as positive ions.

If n_- is not produced by DA to vibrationally excited molecules but, for instance, produced by dissociative attachment to metastable molecules ($c\,^3\Pi_u^-$) with density n_c, one has

$$n_- = n_c n_e\langle\sigma_{cDA}v_e\rangle\tau_-, \tag{12a}$$

or by polar dissociation of hydrogen molecules:

$$n_- = n_p n_g\langle\sigma_{pD}v_p\rangle\tau_-, \tag{12b}$$

Production by DA to metastables can occur both in driver and extraction regions. Production of H^- via polar dissociation of H_2 molecules or H_3^+ ions by primary electrons can of course only take place in the driver region.

III. EXPERIMENTAL SETUP

A. Multicusp ion source

The ion source is a rectangular magnetic-multipole bucket source. The area perpendicular to the beam axis is 14×19 cm^2. The source is 23 cm deep (Fig. 1). This is 9 cm deeper than the source we used for the REMPI measurements.[20] The front plate or beam-forming electrode is electrically insulated from the rest of the walls and can be biased with respect to these walls. Except for the front plate, all walls are equipped with permanent Co-Sm magnets in a line-cusp configuration generating a cusp field of ≈ 0.07 T on the inside. Three sets of two tungsten filaments each are mounted in the backplate. The walls are made of oxygen free copper and covered by a layer of tungsten evaporated from the filaments. The source is operated up to 50 A, 200 V dc. The filling pressure in the source is between 0.2 and 5 Pa. No noticeable change of the pressure measured externally using a Pirani gauge with and without discharge was observed. A magnetic dipole filter was created by two rows of extra magnets on top of the cusp field magnets, as indicated in Fig. 1. By this means a filter was created of 4×10^{-3} T, having a depth of ≈ 2 cm on axis, and extending over the whole area perpendicular on the source axis.

B. Extraction system

The aperture in the 3-mm-thick frontplate has a diameter of 8 mm. At a distance of 3 mm behind the front plate an extraction electrode is mounted (see Fig. 1). It can be biased to a potential of 4 kV positive with respect to the front plate. This electrode, 12 mm thick, consists of two plates in which small magnets are inserted in an octupole configuration (same configuration as applied by Holmes, Dammertz, and Green[21]) to prevent electrons from reaching the detector. The magnetic field strength in the aperture is ≈ 0.1 T. The two plates are insulated from each other, but connected through a 10-kΩ resistor. In case electrons arrive at the second plate, this plate will get a slightly negative potential with respect to the first one, and suppress this electron current. Thus, secondary electrons generated on the first plate are prevented from being accelerated. At a distance of 5 mm behind the extraction electrode the end plate is mounted, behind which, at 30 mm distance, Faraday cups are placed to detect the H^- current. To suppress secondary electron emission, the Faraday cups are biased positively with respect to the environment. All apertures of the electrodes have a diameter of 8 mm. The total acceleration voltage is 15 kV. When running the discharge in argon, no measurable current on the Faraday cups is detected, so electrons do not reach the detector.

The measurements were done as follows. First the heating current through the filaments and the gas flow were turned on. Then, the discharge voltage was switched on. After several seconds the extraction and acceleration voltages were switched on for a time period of 100 ms. During these 100 ms no time dependence was observed in either the H^- current to the Faraday cups or the electron current to the extraction electrode, as measured with a storage scope. Also, no differences in current were observed when the time delay between switching on the discharge voltage and switching on the extraction and acceleration voltage was varied from 1 to 10 s. In almost all measurements, the extraction voltage was chosen sufficiently high to saturate the H^- current to the detector. This occurred at a ratio of total acceleration to extraction voltage of ≈ 7. This agrees with observations in similar sources by Holmes and Green.[22] The electron current on the extraction electrode could be diminished by biasing the beam-forming electrode 1 or 2 V positive with respect to the walls of the source body. Up to 2 V, the H^- current on the Faraday cups showed almost no decrease with this bias voltage. In the measurements presented in this paper no bias voltage was applied.

C. Langmuir probes

The positive ion density n_i, the electron density n_e, and the electron temperature T_e were measured with a Langmuir probe. The probe, a tungsten wire with a diameter of 60 or 175 μm and a length of 3 or 10 mm, respectively, was placed parallel to the front plate. Its position was on the axis

of the discharge chamber, about 3 cm in front of the extraction aperture (see Fig. 1). The probe voltage was swept over a definable range of 80 V at maximum, in a time interval of 4 ms. When dealing with the positive (ion) branch of the probe characteristic, the probe current was measured over a resistor of 1000 Ω in the case where the probe was placed in the extractor and 330 Ω in the case where it was in the driver. When measuring the electron branch, 100- and 33-Ω resistors were used for the extractor and the driver, respectively. The measured probe voltage and current were stored and analyzed using a VAX computer. To obtain both n_i and n_e with sufficient resolution, two sweeps were done. A 30-V sweep was done with zero dc offset and high resolution, to obtain the electron density and electron temperature. The other was done with a dc offset of -40 V and a voltage range of 70 V, to determine n_i.

We use thin cylindrical probes, under all conditions maintaining $R_p/\lambda_d < 6$, where R_d is the probe radius and λ_d the Debye length:

$$\lambda_d = (\varepsilon_0 kT_e/n_e e^2)^{1/2}. \tag{13}$$

To obtain the plasma parameters, the same iterative method was used as that developed by Hopkins and Graham,[23] which is based on the Laframboise theory.[24] In short, using the scaling parameters R_p/λ_d and χ, where

$$\chi = e(V_{\text{probe}} - V_p)/kT_e, \tag{14}$$

with V_p the plasma potential and V_{probe} the probe potential, one can calculate n_e and n_i according to:

$$n_e = \frac{-I_e(\chi)}{eR_p(2\pi kT_e/m_e)^{1/2} f(R_p/\lambda_d,\chi)} \quad \chi > 0 \tag{15}$$

and

$$n_i = \frac{-I_i(\chi)}{eR_p(2\pi kT_e/m_i)^{1/2} f(R_p/\lambda_d,\chi)} \quad \chi < 0. \tag{16}$$

Here $f(R_p/\lambda_d,\chi)$ is a function given by Laframboise.[24] The thermal electron current $I_e(\chi)$ and the ion current $I_i(\chi)$ are related to the probe current $I(\chi)$ according to the relation

$$I_e(\chi) = I(\chi) - I_i(\chi) - I_p(\chi), \tag{17}$$

where $I_p(\chi)$ denotes the current to the probe of fast electrons. All currents are defined per unit length of the probe. T_e is obtained from the exponential region of the probe characteristic corrected for the positive ion current $I_i(\chi)$ and the fast electron current $I_p(\chi)$. V_p is first approximated by the voltage at which the first derivative has its maximum. Then V_p, n_e, T_e, χ, and R_p/λ_d are calculated in an iterative process. To calculate n_i with Eq. (16) we assume the dominant positive ion species to be H_3^+. This looks reasonable since it was measured in a similar source by Holmes *et al.*[25] having parameters similar to our source. In case probe measurements were performed in the driver, n_i was determined by measuring the current to the probe at a fixed value of 20 V negative with respect to the filament voltage. At this voltage primary electrons cannot reach the probe.

The primary electron density n_p was derived in a similar way as described by Hopkins *et al.* In short, using Eq. (17), I_p is calculated for values of $\chi < 10$, as the thermal electron current I_e can be neglected in this region. Then I_p is fitted to

$$I_p = I_{0p} \exp(\chi kT_e/kT_p). \tag{18}$$

The reciprocal of the slope of a least squares logarithmic fit gives T_p. I_{0p} is derived from the abscissa. The use of Eq. (17) for primary electrons yields n_p. Although the fast electron distribution is not a perfect Maxwellian one, it was shown by Hopkins and Graham[23] that this method gives a good estimate of n_p and T_p.

D. Laser detachment

To measure the H^- density, we used the photodetachment technique, as applied to a hydrogen discharge by Bacal and Hamilton.[12] In this method, one measures the increase of the electron current to a positively biased probe due to laser detachment of the H^- ions around the probe. A straight cylindrical probe is placed in the laser beam, but perpendicular to the beam axis (see Figs. 1 and 2).

The cross sections for laser detachment have been measured by Smith and Burch.[26] This cross section does not change much between 600 and 1000 nm. To be sure that other particles in the discharge do not get detached or ionized, and so influence the measured detachment signal, one has to use a long wavelength, or one needs the possibility to vary the wavelength. The group of Bacal[12] has used Ruby and Nd-Yag lasers with fixed wavelength. We have used an excimer-pumped tunable dye laser. First we measured in the

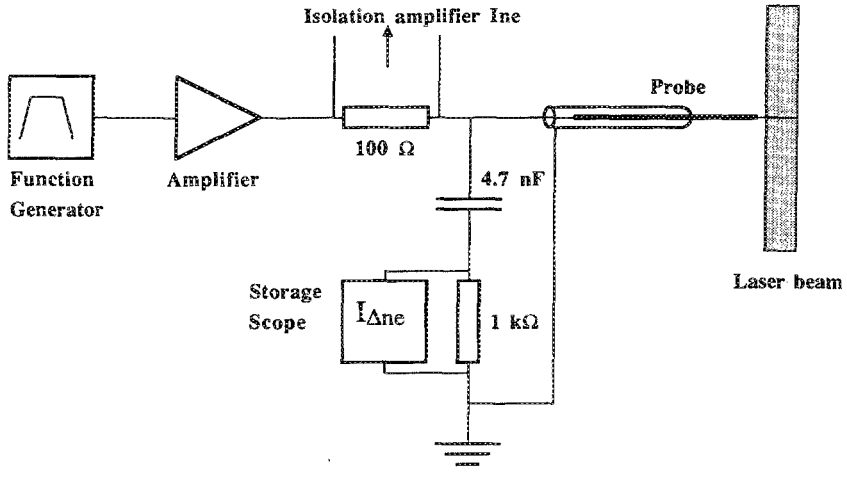

FIG. 2. Schematic drawing of Langmuir probe, laser beam, and probe circuit.

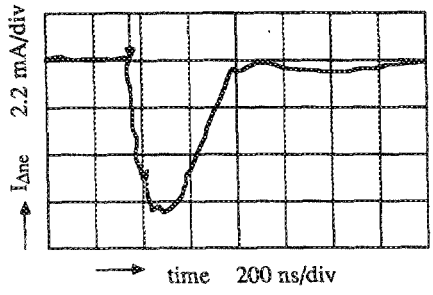

FIG. 3. Scope trace of the detachment signal. Horizontal axis time 200 ns/div, vertical axis voltage over resistor 100 mV/div, discharge current 20 A, discharge voltage 100 V, and source pressure 0.4 Pa.

wavelength range between 690 and 750 nm using Nile Blue as dye solution. Because we did not observe changes in the detachment signal as a function of wavelength, we decided to measure at 725 nm, where the laser dye solution has the largest energy output. In the source chamber, the pulse length of the laser was 15 ns, the pulse energy 12 mJ, and the laser-beam diameter 9 mm.

In Fig. 3 a scope trace of the photodetachment signal is shown. The laser pulse is indicated by the arrow in Fig. 3. If the pulse energy of the laser is high enough to saturate the detachment signal, one does not need to know the cross section for laser detachment. In this case n_{H^-} is proportional to the amplitude of the detachment signal, $I_{\Delta ne}$. We observe saturation of the detachment signal for laser pulse energies larger than ≈ 5 mJ. The electron current to the probe I_e was measured simultaneously with the photodetachment current.

To calculate absolute H^- densities, it is necessary to know n_e and the sum of plasma and primary electron current to the probe I_{ne}. If we assume that the detachment electrons and plasma electrons originate from the same collection area and are detected with the same probability, we can easily calculate n_{H^-}, using the method of Bacal and Hamilton,[12] by setting

$$n_{H^-} = n_e \times I_{\Delta ne}/I_{ne}. \tag{19}$$

This statement needs more attention. Figure 4 gives the ratio of $I_{\Delta ne}/I_{ne}$ as a function of probe voltage. We observe that the ratio of $I_{\Delta ne}/I_{ne}$ increases with probe voltage and saturates above 20 V. Below 10 V the detachment signal, such as measured in Fig. 3, shows a broadening and a rapid decrease of the amplitude $I_{\Delta ne}$. The reason for this broadening is not understood. To be free of probe voltage effects, we have done all our measurements at a voltage of 30 V.

Using an approximation of the Laframboise theory,[24] the collecting radius of the probe is estimated to vary from ≈ 1 mm for $n_e = 10^{10}$ cm^{-3} to ≈ 0.1 mm for 10^{12} cm^{-3}. In the high-density case the measured detachment signal starts to decrease due to a reduction of the collection volume by shadowing of the laser by the probe. At lower plasma densities, this effect also occurs at lower probe voltages. This might explain some of the lowering of $I_{\Delta ne}/I_{ne}$ below a probe voltage of 10 V.

Detached electrons gain the photon energy minus the electron affinity (0.75 eV). For 725 nm this yields an energy T_m of ≈ 1 eV (isotropic velocity distribution). T_e is 0.6 eV for the conditions used in Fig. 4. Since differences in energy between detached and plasma electrons are small, we also expect that their collection radii are similar. Varying the laser energy, we vary the detached electron energy. Using different laser wavelengths (600, 690, 725, and 750 nm), we saw no change in the dependence of $I_{\Delta ne}/I_{ne}$ on probe voltage.

At small probe voltages the amplitude of the detachment signal drops to zero. This occurs when the probe voltage approaches the plasma potential minus the energy of the monoenergetic detached electrons. Below this voltage the detached electrons cannot reach the probe. The phenomena could be used to determine the plasma potential, in a way similar to hot wire probes.[27] However, it is a cumbersome and inaccurate method, and the iterative method described in Sec. III C is much better.

Stern *et al.*[28] have provided an explanation for the duration of the detachment signal, such as shown in Fig. 3. They state that the ratio of the diameter of the laser beam and the duration of the detachment signal is a measure for the drive velocity of H^- in the discharge. We cannot apply this technique with the same accuracy, since we performed our measurements with the probe perpendicular to the laser beam, whereas Stern *et al.*[28] measured with the probe coaxial with the laser beam.

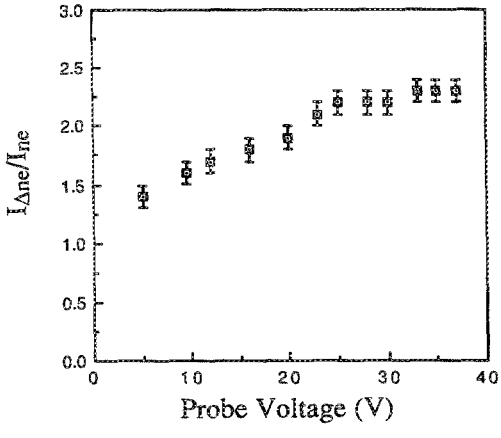

FIG. 4. Ratio of laser detachment signal and dc electron current to the probe as a function of probe voltage. Pressure 0.4 Pa, discharge current 20 A, and discharge voltage 100 V.

IV. EXPERIMENTAL RESULTS AND DISCUSSION

A. Extraction

Figure 5(a) shows a measurement of the extracted H^- ion current I_{H^-} as a function of source pressure for different discharge voltages V_d. At low pressure, we see an increase of I_{H^-} with pressure and subsequently a decrease. Figure 5(b) shows a measurement of I_{H^-} as a function of pressure for different discharge currents I_d. Also here, one observes an increase of I_{H^-} with pressure followed by a decrease. Figure 5 was measured in the source with a magnetic filter. Without the filter the extracted currents were roughly a factor of 2

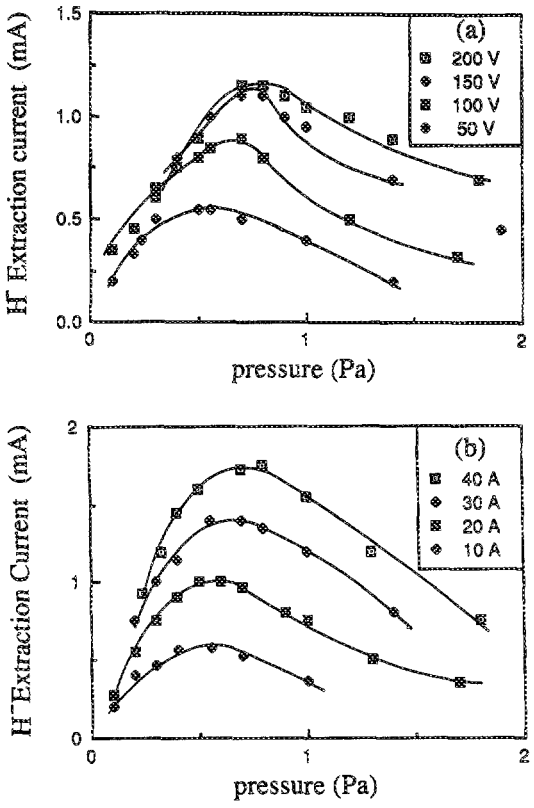

FIG. 5. (a) Extracted H^- current (source with filter) as a function of source pressure for various discharge voltages. Extraction voltage 2 kV. Discharge current 20 A. Bias 0 V. Total acceleration voltage 15 kV. (b) Same as (a) but now for various discharge currents. Extraction voltage 2 kV for 5, 10, and 20 A and 3.3 kV for 30, 40, and 50 A. Discharge voltage 100 V.

smaller. Corresponding data points of Figs. 5(a) and 5(b) show differences of the order of 10%, which fall within experimental error. In fact, they reproduce well if one takes into account that the data were collected on different days of the same week, but with a slightly different setting of the extraction voltage [i.e., extraction voltage 2 kV in Fig. 5(a) and 2.5 kV in Fig. 5(b) for 10 A and 100 V], resulting in a slightly nonoptimized beam transport.

The maximum current density extracted through the aperture of 0.8 cm diameter was 4 mA/cm^2 for a discharge of 50 A, 100 V, and 0.9 Pa. This is small compared to current densities reported by others.[21,29,30] This is due to two effects. First, our filter was not optimized in strength, width, or axial position with respect to the beam-forming electrode. According to measurements of Leung and co-workers[30] and calculations by Hiskes,[15] this can result in a factor of 2–10 loss in I_{H^-}. Second, detachment of H^- will occur during acceleration, due to collisions with neutrals effusing out of the source. Hence, this stripping effect depends on source pressure. Especially in the first accelleration gap, the stripping of the H^- ions in collisions with ground-state molecules is an important phenomenon.[29] Stripping losses can be calculated according to[21]

$$I = I_0 \exp\left(- \int_l n^* \sigma \, dl \right), \tag{20}$$

where I is the measured negative ion current, I_0 is the current emitted by the plasma surface, σ is the cross section for stripping, n^* is the density of particles on which the stripping takes place, and l is the length of the negative ion trajectory. We take into account neutralization of H^- due to collisions with neutral atoms, and due to collisions with neutral molecules. The cross sections for these processes are given in Table I. The axial density profiles of atoms and molecules are calculated from estimated gas conductances of the extractor parts. For this calculation we assume a gas temperature of 300 K. Bonnie and co-workers[11] measured a rotational temperature of 400 K of molecules in the vibrational ground state. The largest uncertainty in this calculation is caused by the rough estimate of the transverse conductances and pressures. Figure 6 shows the result when the data of Fig. 5(b) are in/extrapolated and corrected according to Eq. (20). At a discharge pressure of 1 Pa, $\approx$60% of the H^- ions reaches the detector.

B. H^- density

Figure 7 gives measurements of the H^- ion density, n_-, as a function of gas pressure p for various discharge voltages and currents. All data were obtained with a source equipped

TABLE I. Cross sections and rate coefficients of processes in the discharge and extractor concerning H^-.

Process	Energy	σ (cm^2)	Temperature	Rate (cm^3 s^{-1})	Reference
Production					
DA ($v'' \geqslant 5$)			1 eV	$\approx 2\times10^{-8}$	6
Polar dissociation	40–60 eV	$\approx 3\times10^{-20}$	50 eV	$\approx 1.1\times10^{-11}$	9
DA $c\,^3\Pi u$			1 eV	$< 5\times10^{-10}$	8
Destruction					
$H^- + e_p$	30 eV	3.5×10^{-15}	30 eV	$\approx 1.3\times10^{-6}$	35,15
$H^- + e$			1 eV	$\approx 2\times10^{-8}$	8,15
$H^- + H_x^+$			0.1 eV	$\approx 5\times10^{-8}$	8,15
$H^- + H$			0.1 eV	$\approx 1\times10^{-9}$	9
$H^- + H_2$	$<$0.2 eV	$< 10^{-16}$			38
Accelerator					
$H^- + H$	1–10 eV	8×10^{-15}			36
$H + H$	1 keV	1.4×10^{-15}			34
$H^- + H_2$	1 keV	1×10^{-15}			37

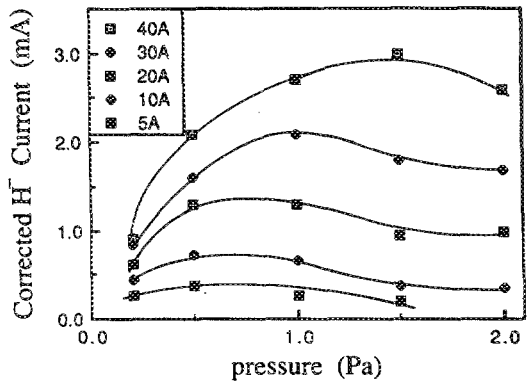

FIG. 6. Extraction current corrected for beam losses calculated from Fig. 5(a).

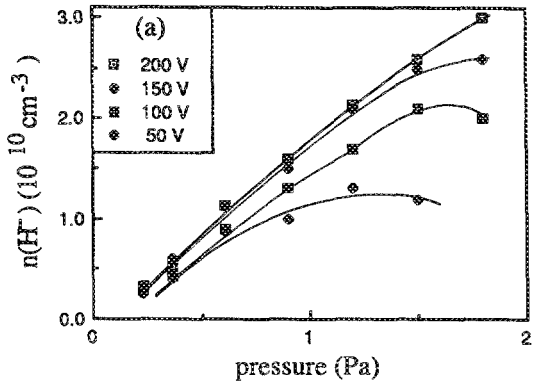

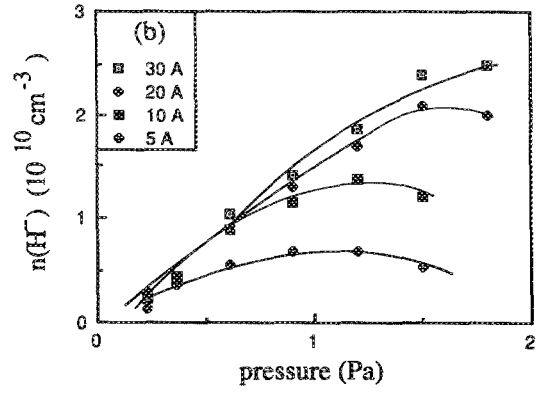

FIG. 8. (a) Absolute H^- density n_- (source without filter) as a function of source pressure for various discharge voltages. Discharge current 20 A. (b) Same as (a) but now as a function of source pressure for various discharge currents. Discharge voltage 100 V.

with a magnetic filter. The fractional H^- density n_-/n_e varies between 5% and 40% in this configuration. As was the case with the H^- extraction measurements, one observes an initial increase with pressure followed by a saturation or a decrease. For larger values of V_d or I_d, the maximum in the n_- curves shifts to higher pressures. Corresponding data points in Figs. 7(a) and 7(b) now show a good agreement. This means that the source conditions as well as the detachment measurement reproduce well.

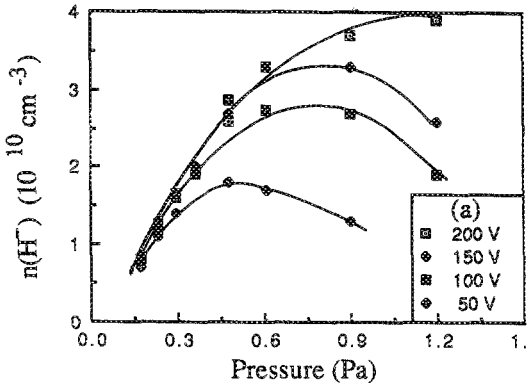

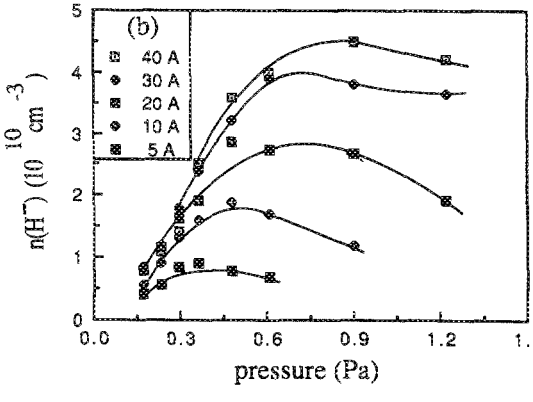

FIG. 7. (a) Absolute H^- density (source with filter) as a function of source pressure for various discharge voltages. Discharge current 20 A. (b) Same as (a) but now as a function of source pressure for various discharge currents. Discharge voltage 100 V.

Figure 8 gives measurements of the H^- ion density as a function of p in the case of a source without a magnetic filter, but with a negatively biased front plate (filament potential), for different discharge voltages and currents. The data show the same qualitative behavior as those in Fig. 7, but the maximum densities have shifted to higher pressures, whereas the maxima themselves have smaller values. These features appear to be more pronounced for smaller discharge voltages. The fractional H^- density n_-/n_e varies between 1% and 8% in the driver. In most conditions, the ratio n_-/n_e is a factor of 4 smaller than in the extractor.

C. Electron and positive ion densities and temperatures

Plasma densities were determined for the two source configurations described earlier. Figures 9(a), 9(b), and 9(c) show the densities of electrons n_e and positive ions n_i as a function of the discharge voltage V_d in the case of a source without magnetic filter and the front plate on filament potential. The densities of the plasma electrons, being between 10^{10} and 10^{12} cm^{-3}, are roughly a factor of 2–4 higher than in the extraction region of a source with filter. This implies that we have a so-called "medium density discharge," for which H_3^+ is estimated to be the dominant positive ion spe-

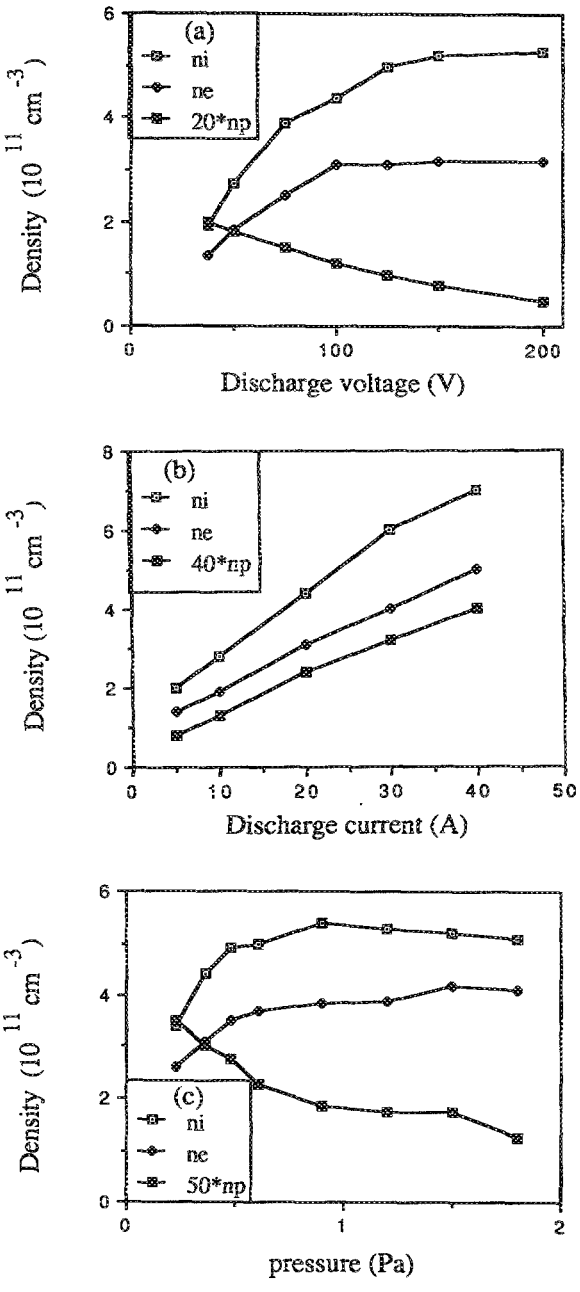

FIG. 9. Electron density and positive ion density as a function of (a) discharge voltage (20 A, 0.4 Pa), (b) discharge current (100 V, 0.4 Pa), and (c) pressure (20 A, 100 V). Source without filter, front plate on cathode potential.

cies.[23,25] This assumption was used in interpretating the probe characteristics. In all measurements the positive ion densities and electron densities show the same qualitative behavior as a function of V_d, I_d, or p, as one expects, but the positive ion densities were roughtly a factor of 1.5 higher than the electron densities. The same effect was measured by Hopkins and Graham.[23] They observed this difference both in a hydrogen discharge and in an argon discharge. So it is unlikely that this effect has anything to do with the existence of negative ions. This is further confirmed by our measurements in the "driver," where we observe that n_- is only 5% of n_e and still find that n_i exceeds n_e by a factor of 1.5. Smith and Plumb[31] measured too high values of n_i in a Kr afterglow plasma using very thin cylindrical probes, and presented a theoretical description that accurately explains the discrepancy. On the basis of their theory (although T_e is much lower in their case), we expect for our source that n_i is a factor of 1.5 too high, provided the positive ions consist for 60% of H_3^+ ions and for 40% of H^+ ions.

The density of primary electrons in the driver has been determined too. In addition, fast electron temperatures have been determined, which were a third of the discharge voltage at pressures between 0.3 and 1 Pa. The values of n_p are shown in Figs. 9(a), 9(b), and 9(c) and Tables I and II. One sees that the density of fast electrons is about 1% of that of the thermal electrons. These observations agree with measurements by Hopkins and Graham.[23]

Measurements of the density and electron temperature in the extractor region (with magnetic filter) are presented in Figs. 10 and 11, respectively. The electron temperature T_e stays below 1 eV and is found to decrease with source pressure, but to increase slightly with increasing discharge voltage or current. We will make use of these measurements in the discussion in Sec. IV D of the drift velocity of H^- ions in the discharge.

D. Drift velocity of H^- ions

To obtain intense low-emittance H^- beams, knowledge of the drift velocity of H^- ions towards the extractor is important. Dividing the corrected extracted current density, Fig. 6, by the negative ion density, Fig. 7(b), we find a measure of this drift velocity. The result is presented in Fig. 12. We observe the following with increasing pressure: First the drift velocity strongly decreases, then it saturates and subsequently it tends to decrease again.

Calculating drift velocities from the duration of the detachment signal, as explained in Sec. II D, yielding velocities for H^- of 11 000 m/s for 40 A, 9000 m/s for 20 A, and 7000 m/s for 5 A, at 0.3 Pa and 100 V. This is slightly higher than the drift velocities calculated from the ratio of corrected extraction current and H^- density. Regarding the fact that we apply two totally different methods to calculate the drift velocity of H^- ions, the drift velocities agree remarkably well.

TABLE II. Plasma parameters and measured densities (cm^{-3}). Gas pressure 1 Pa, discharge voltage 100 V; no filter present, front plate on cathode potential.

I_d (A)	V_{pl} (V)	T_e (eV)	n_p (10^9)	n_e (10^{11})	n_H (10^{13})	$nc^3\pi_u$ (10^9)	$n(0)$ (10^{14})	$n(1)$ (10^{13})	$n(2)$ (10^{12})	$n(3)$ (10^{11})	$n(4)$ (10^{10})	$n(5)$ (10^{10})	n_H (10^{10})
30	3.1	1.4	5.0	6.0	4.2	2.3	0.88	0.95	1.0	1.8	5.7	3.4	1.75
20	2.8	1.3	3.5	4.5	3.0	1.8	0.95	1.0	1.05	2.2	5.8	2.6	1.610
10	2.6	1.0	1.7	3.0	1.5	0.9	1.3	1.2	1.2	2.6	6.5	1.6	1.25
5	2.3	0.8	0.9	2.0	6.7	0.3	1.5	1.25	1.1	2.1	4.0	0.9	5.7

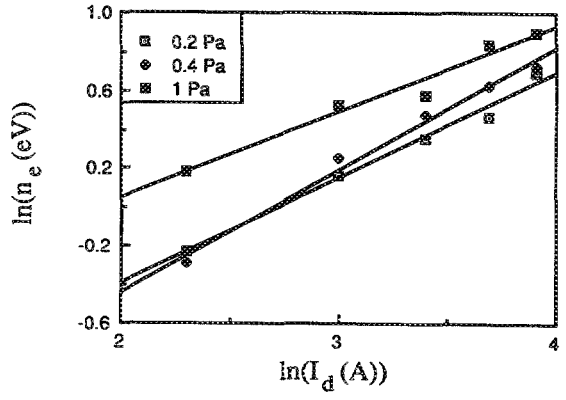

FIG. 10. The logarithm of the electron density as a function of the logarithm of the discharge current for various pressures in the extractor region. The discharge voltage is 100 V. 0.2 Pa $n_e \sim I_d^{0.55}$, 0.4 Pa $n_e \sim I_d^{0.6}$, and 1 Pa $n_e \sim I_d^{0.45}$.

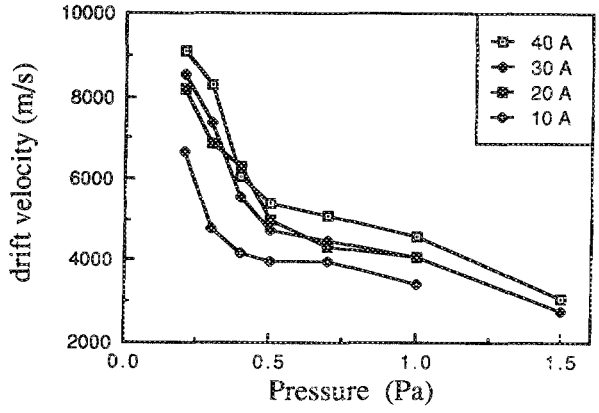

FIG. 12. Drift velocity of H^- ions as a function of pressure for various currents. The discharge voltage is 100 V.

In the following we discuss the results on the drift velocity. The thermal velocity of H^- in the discharge is $(8kT_-/\pi m_i)^{1/2}$. According to calculations of Wadehra and Bardsley[6] the average kinetic energy of H^- ions created by dissociative attachment of $H_2(v'')$ increases from 0.2 to 0.4 eV ($\approx$7000 to $\approx$10.000 m/s) when the electron energy increases from 0.4 to 1.5 eV. In the extraction region T_e stays below 1 eV for all discharge conditions [see Fig. 11(b)]. This implies that the observed drift velocities are very close to the H^- ion velocities, resulting from dissociative attachment.

It can be expected that the charged plasma particles in the driver exhibit a drift toward the front plate, where they are destroyed, either by wall neutralization or by extraction. It is known that positive ions enter the sheath of the extraction region with the ion acoustic velocity, the so-called Bohm sheath criterion. This was confirmed in extraction measurements of positive ions. The ion acoustic velocity,

$$v_a = [(kT_e + 3kT_i)/m_i]^{1/2} \approx 7000 \text{ m/s}$$

for T_e of 0.5 eV. Here it is assumed that the ion temperature equals the gas temperature. If H^- ions participate in this drift, then their drift velocity could be equal to the positive ion acoustic velocity and scale with $\sqrt{T_e}$. Figure 13 presents a plot of the negative ion drift velocity and the ion acoustic velocity as a function of discharge current, calculated with the measured electron temperatures [Fig. 11(b)], for a discharge with discharge voltage and pressure equal to 100 V and 0.2 Pa. Although there are differences between the drift

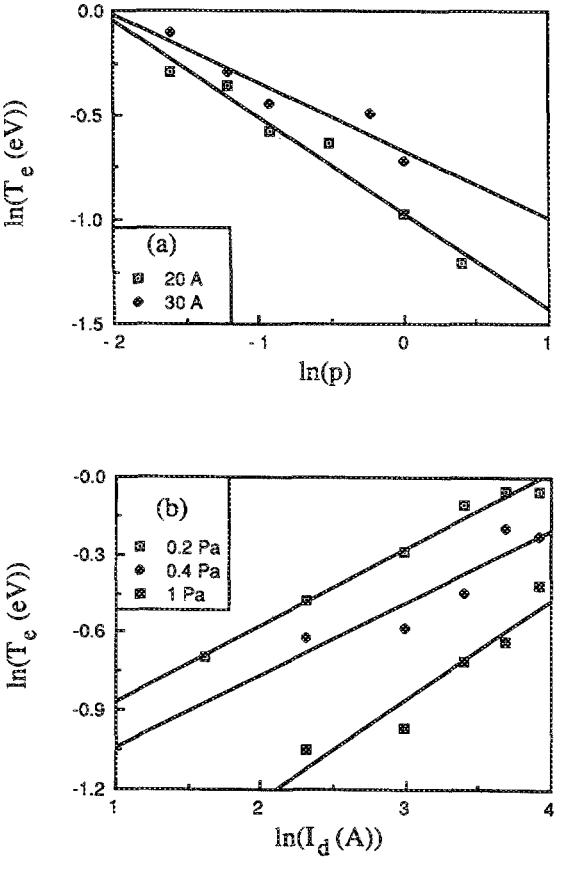

FIG. 11. (a) The logarithm of the electron temperature as a function of the logarithm of pressure for 20 and 30 A in the extractor region. The discharge voltage is 100 V. Scaling T_e: 20 A, $T_e \sim p^{-0.45}$ and 30 A, $T_e \sim p^{-0.3}$ and (b) $\ln(T_e)$ as a function of discharge current for various pressures (100 V). 0.2 Pa $T_e \sim I_d^{0.3}$, 0.4 Pa $T_e \sim I_d^{0.3}$, and 1 Pa $T_e \sim I_d^{0.4}$.

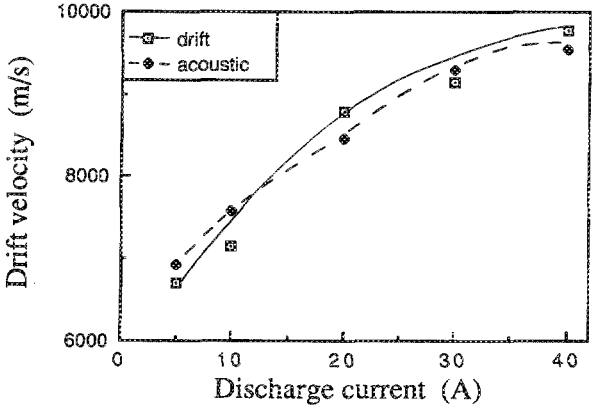

FIG. 13. Drift velocity of H^- ions as a function of discharge current (100 V and 0.2 Pa). The drawn curve is the ion acoustic velocity.

velocity and the ion acoustic velocity of 20%, caused by the strange dip in the drift velocities between 0.4 and 0.8 Pa, a scaling of the drift velocity with the ion acoustic velocity was observed for all measurements as a function of pressure and discharge current. Contrary to observations on the hybrid multipole source, reported by Bacal *et al.*,[32] our measurements show a scaling of the drift velocity with $\sqrt{T_e}$. Bacal *et al.*[32] observed no dependence of the H^- drift velocity on T_e.

The accuracy of the measurements does not permit us to choose between both possibilities. However, the $\sqrt{T_e}$ dependence is suggestive of an ambipolar diffusion-induced drift. Further, it leads to the conclusion that it is advantageous to keep the electron temperature as low as possible. Then H^- ions are formed with a low thermal velocity, resulting in a small beam divergence.

E. Ionization of other particles by laser detachment

We attempted to investigate the presence of other particles in the discharge, such as metastables, by means of a laser ionization technique. Bonnie and co-workers[14] have shown that outside the discharge it is possible to detect metastable molecules ($c\,^3\Pi_u$) by a one-photon excitation, one-photon ionization scheme [(1 + 1) Resonant Multiphonon Ionization (RMI), photon wavelength $\approx$600 nm], using one of the electronically highly excited triplet states ($g^3\Sigma_g^+$, $h\,^3\Sigma_g^+$, $i^3\Pi g$, $j^3\Delta g$) as an intermediate state. With direct one-photon ionization (wavelength 337 nm), Bonnie and co-workers[14] obtained a lower limit for the density of metastables in the discharge of $\approx 10^9$ cm^{-3}. When the laser frequency resonates with some transition in a molecule, the molecule is ionized and a probe may detect the excess electrons, similar to laser detachment of H^- ions. We carefully scanned the laser wavelength between 580 and 610 nm, but we did not see any resonance in the current to a positively biased probe. This was done in both source configurations. We ascribe this to the fact that the H^- detachment signal ($n_- \approx 2\times 10^{10}$ cm^{-3}) dominates the (1 + 1)RMI signal of the metastables. If we assume that we can saturate the (1 + 1) transition of the metastables, and that we can detect a 5% change in the detachment signal, we obtain an upper limit for the density of metastables of $\approx 10^9$ cm^{-3} molecules in a specific vibrational and rotational state. Because the total density, after summing over all internal degrees of freedom, is expected to be $\approx 10^9$ cm^{-3}, the method does not have the required sensitivity. Conversely, we conclude that the detachment signal is not perturbed by the ionization of other particle species at the laser intensities used.

Since we were not able to detect electrons formed by ionization of metastables, we tried to detect positive ions. Laser detachment of H^- will not produce positive ions. Of course the positive ion current to a Langmuir probe is much lower than the electron current at the same density due to the difference in mobility. Also, a possible positive current will have a longer time duration, further decreasing the amplitude. However, due to noise caused by the ignition of the excimer laser discharge, we could not obtain reproducible signals.

V. APPLICATION OF MODEL TO OUR SOURCE

A. Plasma density

The increase and saturation of the plasma density with pressure in all source configuration is understood on the basis of Eq. (7). The plasma density does not increase linearly with discharge current, since part of the energy put into the discharge is used to increase the electron and ion temperature. This can be shown by plotting the product of plasma density n_e and electron temperature T_e as a function of I_d. Although not shown here, this gives a straight line, a scaling law earlier shown by Hopkins and Graham.[33] The plasma density also increases with discharge voltage V_d, since the ratio $\langle\sigma_{\rm ion} v_p\rangle/\langle\sigma_{in} v_p\rangle$ will increase with V_d up to 100 V and then saturates at higher voltages. This is can be seen in Fig. 9(a).

B. H⁻ density

First we discuss the dependence of n_- on discharge parameters in the geometry with positively biased front plate and with magnetic filter qualitatively. Then we discuss n_- in the configuration without filter and the front plate on cathode potential quantitatively, by comparing n_- with calculations, using Eqs. (8) and (11) and other measured quantities, such as n_p, n_e, n_i, $n_{\rm H}$, and n''. Different rates and cross sections necessary for these calculations are listed in Table I. The densities necessary to calculate the H^- density are listed in Tables II and III. The values listed in these tables are for the source configuration with the front plate on cathode potential. In Fig. 14 the measured densities of all different species given in Table II are shown.

In Fig. 7 (with magnetic filter, T_e low) it is observed that n_- rises to a maximum and thereafter decreases with pressure. This decrease can be explained using Eqs. (8) and (11). The destruction of n^- at very low pressure is explained by loss of H^- by diffusion to the walls. Other destruction

TABLE III. Plasma parameters and measured densities (cm^{-3}). Discharge current and voltage 10 A and 100 V, respectively; no filter present, front plate on cathode potential.

p (Pa)	$V_{\rm pl}$ (V)	T_e (eV)	n_p (10^9)	n_e (10^{11})	$n_{\rm H}$ (10^{13})	$nc^3\pi_u$ (10^9)	$n(0)$ (10^{14})	$n(1)$ (10^{12})	$n(2)$ (10^{11})	$n(3)$ (10^{11})	$n(4)$ (10^{10})	$n(5)$ (10^{10})	$n_{\rm H}$ (10^9)
0.3	3.2	1.6	4.0	1.8	0.8	1.4	0.375	3.6	3.9	0.87	2.7	0.8	3.5
0.6	2.9	1.3	3.0	2.6	1.0	1.3	0.75	6.9	7.3	1.6	4	1.1	8.5
1.0	2.6	1.0	1.7	3.0	1.5	0.9	1.3	12	12	2.6	6.5	1.6	12
2.0	2.0	0.7	0.7	3.0	0.23	0.4	2.5	21	20	4.3	6.9	1.3	8.0

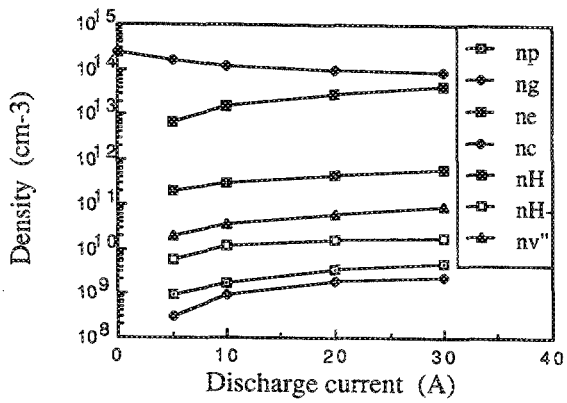

FIG. 14. Densities of all measured species as function of discharge current (Table II, 100 V and 1 Pa). n_c denotes the density of metastables.

processes dominate at higher pressure. Fast electrons are not present in the extraction area and the electron temperature is too low (<1 eV) to have a dominant influence on the H^- density. Loss of H^- by diffusion to the walls can neither explain a decrease on n_- with pressure. Bacal and Hamilton[12] showed that diffusion of H^- to the walls could only have a major effect at electron densities $\leqslant 10^{10}$ cm^{-3}. This is only the case at very low pressure. Since n_i saturates with gas pressure, positive ions cannot explain a decrease of n_- with pressure in our discharge either. It is assumed that $n(v''=5)$ does not decrease dramatically with increasing pressure. This seems reasonable since we did not observe such a decrease with increasing pressure for $n(v''=5)$ in the configuration with the front plate on cathode potential.[10] We did observe that n_H does increase with gas pressure.[10] Thus, loss of H^- by associative detachment can explain the decrease of n_- with pressure in this source geometry. These processes can also explain the almost linear increase of n_- with discharge current at optimum pressure. The densities of the species involved with the production of H^-, n'', and n_e both increase almost linearly with current, whereas n_H and n_i increase also almost linearly with current. The result is an almost linear increase of n_- with discharge current.

In the geometry without magnetic filter and front plate on cathode potential, the H^- density saturates with pressure. These measurements on the H^- density can be discussed in terms of our measurements on the densities of vibrationally excited molecules.[10] H^- densities are calculated

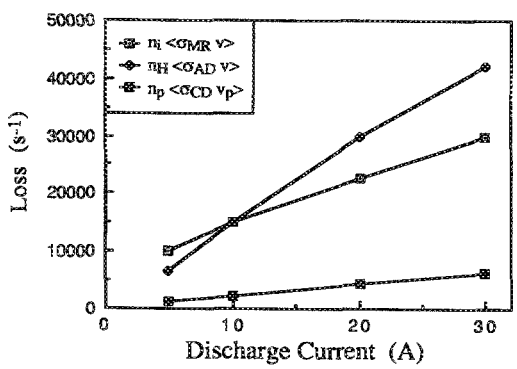

FIG. 15. Various H^- destruction terms as a function of discharge current (100 V and 1 Pa).

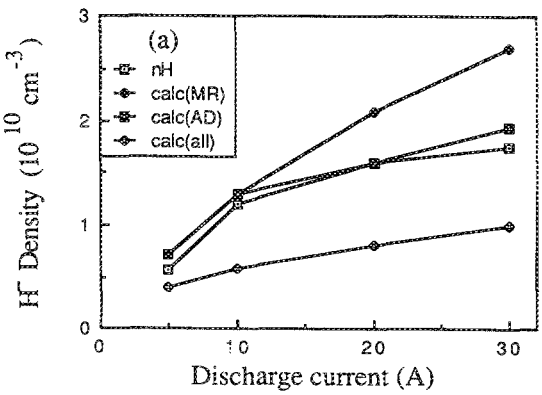

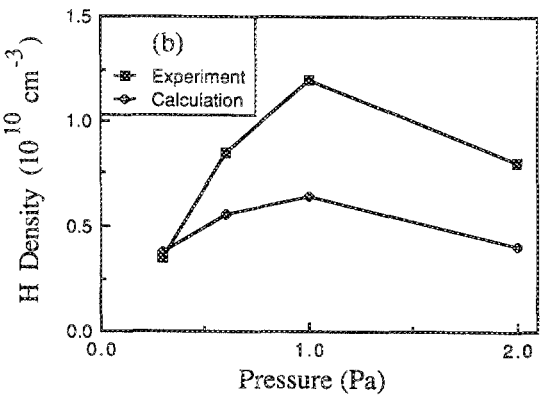

FIG. 16. (a) Experimental and calculated H^- densities as a function of discharge current (100 V and 1 Pa). (b) The same as (a) but now as a function of pressure (10 A and 100 V). The experimental H^- densities are derived from Fig. 8(b).

by substituting the values for the densities of vibrationally excited molecules, of atoms, of primary and of plasma electrons, of positive ions, and the values for the cross sections and rates listed in Table I in Eqs. (8) and (11). The calculations show that the loss by atom collisions $n_H\langle\sigma_{AD}v_H\rangle$ and positive ions $n_i\langle\sigma_{MR}v_i\rangle$ are comparable. Figure 15 shows the most important destruction terms in Eq. (11) as a function of current. Figure 16 shows the measured and calculated n_- as a function of current and pressure, respectively. In the calculations of n_-, we took two times the $n(v''=5)$ density, as a measure of n'' $(4<v''<10)$. This seems reasonable, if we extrapolate the vibrational densities presented in Figs. 5 and 6 in a separate paper.[10] The qualitative agreement is good, so the processes, which we took into account, can explain the experimental data qualitatively well. However, the calculated H^- densities in Fig. 16 are a factor of 2 lower than the measured densities. This may be due to three reasons: (1) The estimate of n'' by two times the $v''=5$ density is too pessimistic; (2) the estimate of the atomic density (upper limit[11]) is too high; and (3) other production processes may contribute to the production of H^-. Additional production processes are DA of electrons to metastables or polar dissociation of H_2 or H_3^+ by primary electrons. Qualitatively, Eq. (12a), production of H^- via dissociative attachment of an electron to metastables, cannot describe the measurements. At higher pressures n_e saturates and n_c de-

creases.[14] Since at higher pressures the destruction processes given in Eq. (11) saturate or decrease, one would expect n_- to decrease as fast or faster than n_e with increasing pressure. This contradicts our measurements. Furthermore, the production term of H^-, $n_c n_e \langle \sigma_{cDA} v_e \rangle$, is a factor of 100 lower than $n'' n_e \langle \sigma_{DA} v_e \rangle$, due to the low density of metastables ($n_c < 3 \times 10^9 \text{ cm}^{-3}$) (Ref. 14). Polar dissociation [Eqs. (3) and (12b)] contributes less than 10% to the production of H^-. Hiskes and Karo[9] remark that polar dissociation may play a role at plasma densities $> 10^{12} \text{ cm}^{-3}$.

VI. CONCLUSIONS

The positive ion density and the electron density increase and saturate with pressure and discharge voltage. This is in agreement with a qualitative model based on rate equations.

Extraction measurements and H^- density measurements were performed in a discharge without filter and with the front plate at filament potential. For low pressures (assuming 30% loss by gas collisions) this gives a drift velocity of $\approx$7000 m/s for H^-. This drift velocity is found to be compatible with both the thermal velocity of H^- and the ion acoustic speed.

The H^- density increases at low pressures and saturates or decreases at higher pressures. Without the magnetic filter the H^- density is proportional with pressure and then saturates. This can be explained by a qualitative model in which H^- is mainly produced by dissociative attachment of thermal electrons to vibrationally highly excited molecules. Saturation of n_- at these pressures means that H^- is predominantly quenched by discharge-produced particles such as electrons, positive ions, and H atoms. The model is further supported by calculations based on rate equations.

The measurements and calculations exclude production of H^- by dissociative attachment of thermal electrons to metastable molecules or polar dissociation under the studied discharge conditions as dominant processes.

Note added in proof. Dr. D. A. Skinner of the Ecole Polytechnique at Palaiseau, France, brought to our attention that an error might have occurred in the wiring of the filaments. After inspection this turned out to be the case. As a consequence, the primary electron energy is 5–15 eV higher than indicated in this and previous work.[10] This leads to a degradation of the confinement of the fast electrons, when the source is operated without magnetic filter. We thank Dr. Skinner for bringing this to our attention.

ACKNOWLEDGMENTS

We wish to thank M. Hopkins (Ulster, Dublin) for advising us about the probe measurements and P. Dijkstra for his technical assistance. This work is part of the research program of the association agreement between EURATOM and the Stichting voor Fundamental Onderzoek der Materie (FOM) with financial support from the Nederlandse Organisatie voor Wetenschappelijk Onderzoek (NWO) and EURATOM.

[1] H. J. Hopman and the NET Team, in *Proceedings of the 3rd European Conference on the Production and Application of Light Negative Ions,* Amersfoort, The Netherlands, 1988, edited by H. J. Hopman and W. v. Amersfoort, Amsterdam (1988), p. 3.
[2] M. Bacal, A. M. Bruneteau, and M. Nachman, J. Appl. Phys. **55**, 15 (1984).
[3] A. J. T. Holmes, L. M. Lea, A. F. Newman, and M. P. S. Nightingale, Rev. Sci. Instrum. **58**, 223 (1987).
[4] K. W. Ehlers, J. Vac. Sci. Technol. A **1**, 974 (1983).
[5] J. R. Hiskes, Comments At. Mol. Phys. **19**, 59 (1987).
[6] J. M. Wadehra and J. N. Bardsley, Phys. Rev. Lett. **41**, 1795 (1978) and Phys. Rev. A **20**, 1398 (1979); J. P. Gauyacq, J. Phys. B **18**, 1859 (1985).
[7] M. Allan and S. F. Wong, Phys. Rev. Lett. **41**, 1791 (1978).
[8] J. R. Hiskes, M. Bacal, and G. W. Hamilton, Lawrence Livermore Laboratory Report No. UCID-18031, 1979 (unpublished).
[9] J. R. Hiskes and A. M. Karo, J. Appl. Phys. **56**, 1927 (1984).
[10] P. J. Eenshuistra, R. M. A. Heeren, A. W. Kleyn, and H. J. Hopman, Phys. Rev. A **40**, 3613 (1989).
[11] J. H. M. Bonnie, P. J. Eenshuistra, and H. J. Hopman, Phys. Rev. A **37**, 1121 (1988).
[12] M. Bacal and G. W. Hamilton, Phys. Rev. Lett. **42**, 1538 (1979).
[13] A. J. T. Holmes, Rev. Sci. Instrum. **53**, 1517 (1982) and Rev. Sci. Instrum. **53**, 1523 (1982) and K. W. Ehlers and K. N. Leung, Rev. Sci. Instrum. **52**, 1452 (1981).
[14] J. H. M. Bonnie, P. J. Eenshuistra, and H. J. Hopman, Phys. Rev. A **37**, 4407 (1988).
[15] J. R. Hiskes, AIP Conf. Proc. No. **158**, 208 (1987).
[16] J. R. Hiskes, A. M. Karo, M. Bacal, A. M. Bruneteau, and W. G. Graham, J. Appl. Phys. **53**, 3469 (1982).
[17] C. Gorse, M. Capitelli, M. Bacal, J. Bretagne, and A. Lagana, Chem. Phys. **117**, 177 (1987).
[18] A. P. H. Goede and T. S. Green, Phys. Fluids **25**, 1797 (1982).
[19] K. N. Leung, R. D. Collier, L. B. Marshall, T. N. Gallaher, W. H. Ingham, R. E. Kribel, and G. R. Taylor, Rev. Sci. Instrum. **49**, 321 (1978).
[20] J. H. M. Bonnie, E. H. A. Granneman, and H. J. Hopman, Rev. Sci. Instrum. **58**, 1353 (1987).
[21] A. J. T. Holmes, G. Dammertz, and T. S. Green, Rev. Sci. Instrum. **56**, 1697 (1985).
[22] A. J. T. Holmes and T. S. Green, AIP Conf. Proc. No. **111**, 429 (1984).
[23] M. B. Hopkins and W. G. Graham, Rev. Sci. Instrum. **57**, 2210 (1986).
[24] J. G. Laframboise, University of Toronto, Institute for Aerospace Studies Report No. 100 (1966) (unpublished).
[25] A. J. T. Holmes, G. Dammertz, T. S. Green, and A. R. Walker in *Proceedings of the International Ion Engineering Congress* (Institute of Electrical Engineers of Japan, Kyoto, 1983), p. 71, and C. F. Chan, C. F. Burrel, and W. S. Cooper, J. Appl. Phys. **54**, 6119 (1984).
[26] S. J. Smith and D. S. Burch, Phys. Rev. **116**, 1125 (1959).
[27] R. H. Huddlestone and S. L. Leonard, Eds., *Plasmadiagnostic Techniques* (Academic, New York, 1965), p. 183.
[28] R. A. Stern, M. Bacal, P. Devynck, and F. Hillon (private communication).
[29] R. McAdams, A. J. T. Holmes, A. F. Newman, and R. King, in *Proceedings of the 3rd European Conference on the Production and Application of Light Negative Ions,* Amersfoort, The Netherlands, 1988, edited by H. J. Hopman and W. v. Amersfoort, Amsterdam, (1988), p. 15; C. F. A. van Os, A. W. Kleyn, L. M. Lea, A. J. T. Holmes, and P. W. van Amersfoort, Rev. Sci. Instrum. **60**, 539 (1989).
[30] K. N. Leung, K. W. Ehlers, and R. V. Pyle, Rev. Sci. Instrum. **56**, 364 (1985).
[31] D. Smith and I. C. Plumb, J. Phys. D **6**, 196 (1973).
[32] M. Bacal, J. Bruneteau, P. Devynck, and F. Hillion, in *Proceedings of the 2nd European Conference on the Production and Application of Light Negative Ions,* Amersfoort, edited by M. Bacal and C. Mouttet (Ecole Polytechnique, Palaiseau, France, 1986), p. 201.
[33] M. B. Hopkins and W. G. Graham, Vacuum **36**, 873 (1986).
[34] R. K. Janev and A. R. Tancic, J. Phys. B **4**, 219 (1971).
[35] B. Peart, D. S. Walton, and K. T. Dolder, J. Phys. B **3**, 1346 (1970).
[36] R. J. Bienek, J. Phys. B **13**, 4405 (1980).
[37] J. S. Risley and R. Geballe, Phys. Rev. A **9**, 2485 (1974).
[38] M. S. Huq, L. D. Doverspike, and R. L. Champion, Phys. Rev. A **27**, 2831 (1983).